RSC Advances

COMMUNICATION

View Article Online
View Journal | View Issue

Cite this: *RSC Adv.*, 2016, **6**, 54281

Facile tailoring of the two-dimensional graphene oxide channels for gas separation†

Jie Shen, Mengchen Zhang, Gongping Liu and Wanqin Jin*

Received 1st April 2016
Accepted 18th May 2016

DOI: 10.1039/c6ra08441a

www.rsc.org/advances

This work demonstrates a facile method of finely tailoring the graphene oxide (GO) nanochannels by controlling their surface oxygenated functionalities. The as-prepared membrane with subnanometer interlayer nanochannels (0.36 nm) and CO_2-philic properties showed excellent preferential CO_2 permeation performance, which offers promising potential for CO_2 capture.

Two dimensional graphene-based materials with unique atomic thickness and excellent mass transport properties are gaining heightened attention for the development of a new family of separation membranes.[1] As a derivative of graphene, graphene oxide (GO) is now considered as a promising nano-building block for membranes, owing to its tunable microstructures and physiochemical properties as well as large-scale fabrication using a solution-based strategy.[2] Through facile oxidization and exfoliation of bulk graphite, a large number of oxygenated functionalities can be chemically bonded on both basal planes and sheets edges of carbon layers,[3] endowing the two dimensional (2D) GO nanosheets with rich chemistry property. As a result, it has been well demonstrated[1,4–7] that GO-based membranes with well-assembled laminar structure can be engineered to provide nanochannels for selective molecular transport. This leads to a success application of GO-based membranes in water treatment due to the highly hydrophilic characteristic.[4–10] Generally, separation properties of membrane can be finely tuned by materials nanostructure.[11] As a result, most of the studies focused on controlling the stacking structure of GO laminates to optimize the membrane separation performance. After being dispersed in water solution, GO nanosheets are assembled into laminates using methods based on mechanical external forces such as dip-coating,[12] filtration[13] and spin-coating.[14] However, it has been proven that the intrinsic repulsive electrostatic forces between the carboxyl groups of GO layers can cause inevitable local disordered stacking structure during GO assembly process.[2] Non-selective defects are then generated, which is negative for effective separation.

Generally, the interlayer space of 2D GO nanosheets has been demonstrated to provide nanochannels for selective molecular transport.[10,15–18] However, it still remains a great challenge to finely regulate the 2D interlayer nanochannels for precise molecular separation of small molecules, such as water desalination and gas sieving. Being different with the methods based on mechanical external forces, in this work, we applied chemical strategy of finely tailoring the GO-derived nanochannels by controlling their surface oxygenated functionalities (Fig. 1). Indeed, the size of GO-derived diffusion nanochannels (interlayer space) is dominated by the amount of oxygen-containing groups on GO nanosheets.[19] Through the method of controllably removing the oxygenated groups, the GO nanochannels can be manipulated to subnanometer for highly-selective gas transport. Moreover, serving as a Lewis acid or a Lewis base, CO_2 molecules can strongly interact with oxygenated groups on GO, especially hydroxyl and carboxy.[17,20] Hence, the interactions between GO nanochannels and CO_2 molecules is expected to be significantly influenced by oxygen-containing groups, which is the critical factor for tuning the CO_2 adsorption behaviors in 2D GO nanochannels. Herein, this proposed bottom-up strategy focusing on improving membrane fabrication from origin, is considered to be easily controlled and scaled up, which can also be extended to other two-dimensional materials membranes.

We prepared GO nanosheets by modified Hummer's method.[3] Subsequently, a lot of oxygenated groups were incorporated onto GO layers, such as epoxy, hydroxy, carbonyl, and carboxy groups. These polar groups enable the stable dispersion of GO in solvent (Fig. 2a). The single or double-layered GO nanosheets were with the thickness of 1–2 nm and lateral size of 1–2 μm (Fig. 2b), which is proved to be suitable for embedding GO nanosheets into polymeric environment to fabricating GO–

State Key Laboratory of Materials-Oriented Chemical Engineering, Nanjing Tech University (former Nanjing University of Technology), 5 Xinmofan Road, Nanjing 210009, P. R. China. E-mail: wqjin@njtech.edu.cn

† Electronic supplementary information (ESI) available: Detailed experimental procedure and supplementary figures and tables. See DOI: 10.1039/c6ra08441a

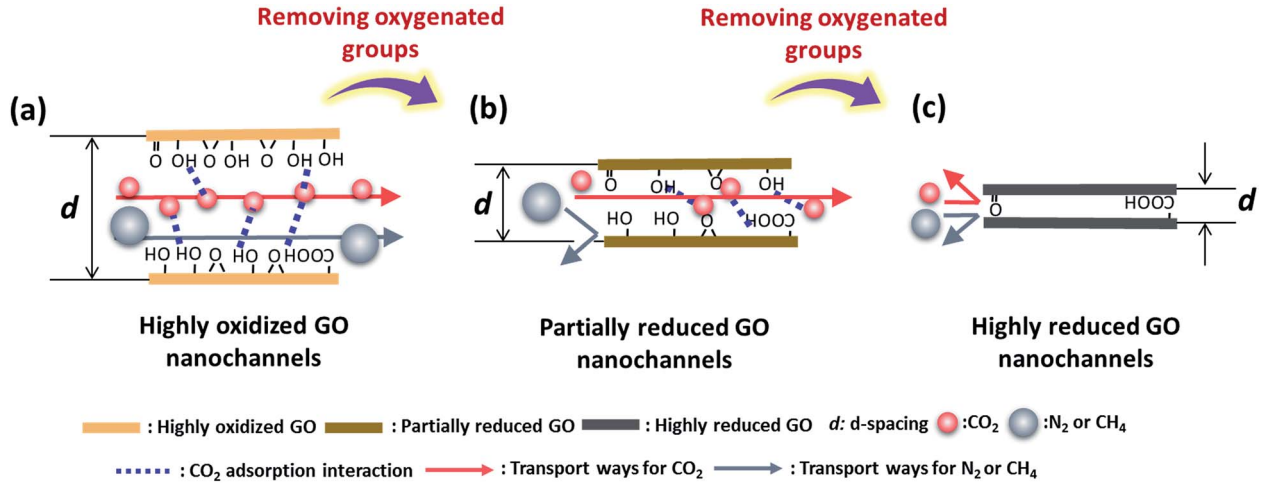

Fig. 1 Schematic of the microstructures and molecular transport mechanisms of two dimensional GO nanochannels with controlled oxygenated groups.

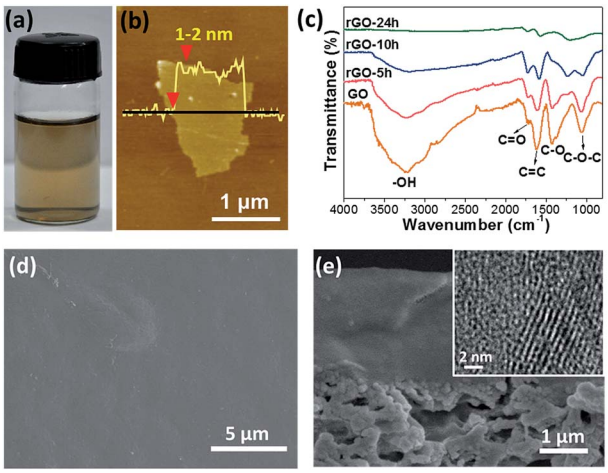

Fig. 2 (a) GO dispersed in water and ethanol mixed solvent with concentration of 0.1 mg mL^{-1}. (b) AFM image of single or double-layered GO. (c) FTIR spectra of GO and reduced GO. (d) Top-view SEM images of GO-0.55 membrane. (e) Side-view SEM images of GO-0.55 membrane with inserted TEM image showing the 2D nanochannels formed in membrane.

polymer membranes.[17] Controlling the amount of oxygenated groups can be realized by gradually reduction of original highly oxidized GO using methods of chemical reduction, intercalation or thermal annealing.[21] However, the former two methods also produce large amount of heteroatoms, which will significantly disrupt the ordered GO stacking structure as well as the interfacial properties between GO and polymer chains, thus to influence the dispersibility of GO in polymeric environment. Therefore, a facile thermal annealing method (see the details in ESI†) on the basis of the analysis of the thermal properties of GO (Fig. S1†) was carried out to obtain reduced GO by controllably removing the oxygen-containing groups. GO powders were reduced under 180 °C for 5, 10 and 24 h, which were denoted as rGO-5 h, rGO-10 h and rGO-24 h, respectively. Fig. 2c showed that oxygen-containing functionalized groups were gradually lost during the thermal reduction process. In addition, as proven by X-ray photoelectron spectroscopy (XPS, Fig. S2†), epoxy and hydroxyl groups occupy the majority of these functionalized groups on GO. After thermal annealing, the amount of epoxy and hydroxyl groups were sharply reduced while carbonyl and carboxy groups were not obviously removed. GO with different O/C ratios of 0.23, 0.41, 0.55 and 0.65 were finally obtained. Thermal annealing under higher temperature (usually up to 400 °C) is effective to remove almost the oxygen-containing groups, forming restored π-conjugated structure, however, it can also cause severe irregular restacking of graphene sheets in polymeric environment due to the prevailing van der Waals interaction.

GO with rich surface chemistry property can easily interact with polymer chains owing to the compatible interfacial properties. This enables the highly efficient self-assembly of GO nanosheets in polymeric environment to fabricate membranes. We selected polyether block amide (PEBA) as the polymer, owing to its abundant functional groups such as –N–H–, H–N–C=O, and O–C=O. Then, GO with different O/C ratios of 0.23, 0.41, 0.55 and 0.65 were dispersed in mixed solvent of water and ethanol ($\omega_{ethanol} : \omega_{water} = 70 : 30$) to fabricate membranes, which can be denoted as GO-0.23, GO-0.41, GO-0.55 and GO-0.65, respectively. For comparison, pure PEBA membrane was also fabricated. Digital images of dense membranes containing GO with different O/C ratios were shown in Fig. S3.† The change of membrane color indicates the difference of GO O/C ratios. It can be seen that GO at low O/C ratio caused visible local aggregation in polymer membrane. Compared with the surface scanning electron microscope (SEM) images of pure PEBA membrane in Fig. S4,† GO-0.55 membrane showed corrugated surface with some bulges on it (Fig. 2d). The as-prepared membrane with rough surface demonstrated the presence of GO laminates [see atomic force microscope (AFM) images in Fig. S5†]. Side-view SEM images clearly showed bulk-like section, which can be ascribed to the presence of the stacked

GO laminates in PEBA layer, with the size of 1–2 μm that is in agreement of AFM characterization shown in Fig. 2b. This can be further confirmed by TEM characterization as shown in Fig. 2e. GO nanosheets assembled into well-defined laminar structure with subnanometer interlayer nanochannels. By varying O/C ratios of GO, the membranes microstructures as well as physicochemical properties were quite different. GO–polymer interactions at interface are considered to be dominated by the state of oxygenated groups that provide interaction sites for interlocking GO nanosheets with polymer. Thus, GO nanosheets can assemble into well-defined GO laminates. As proven by thermogravimetric analysis (TGA) in Fig. S6,† the decomposition temperature of PEBA was obviously improved when GO was with high O/C ratio, indicating that thermal stability was enhanced owing to the strong hydrogen bonding framework. These were further demonstrated by XPS characterization (Fig. S7†), showing a regular shift to higher binding energy for O 1s characteristic peaks by increasing the GO O/C ratio. This demonstrated the decreased electron cloud density of O atoms, suggesting that the hydrogen bonding frameworks can be constructed between O atoms and H atoms.[22] It is reasonable that highly interlocked GO–polymer microstructure was established by increasing the amount of oxygenated groups on GO. On the contrary, GO with low O/C ratio causes weak GO–polymer interaction, which also leads to poor dispersibility of GO nanochannels in polymeric environment.[23]

Indeed, these nanochannels are directly manipulated by the interlayer spacing of GO nanosheets. Fig. 3a exhibits the *d*-spacing of GO with different O/C ratios. It can be found that more oxygenated groups on GO can lead to obviously larger *d*-spacing. The *d*-spacing is considered to be composed of the thickness of single-layer carbon (0.34 nm) and the empty space between adjacent GO layers.[4,5] For GO with O/C ratios of 0.23 and 0.41, the interlayer empty space can be calculated to 0.04 and 0.27 nm, respectively, which can hardly allow any molecules to pass through. Fortunately, after increasing O/C ratio to 0.55, the interlayer empty space rose to approximately 0.36 nm [between the kinetic diameter of CO_2 (0.33 nm) and N_2 (0.364 nm)], which served as the nanochannels for molecular sieving transport. However, with the highest O/C ratio of 0.65, the interlayer empty space was enlarged to 0.5 nm, which is too large for selective diffusion of gas molecules. The enlarged interlayer empty space is believed to increase the gas permeability.

It has been well demonstrated that oxygenated groups on GO can significantly influence the adsorption ability of gas molecules in GO-based membrane, leading to distinct gas permeation behaviors. As proven by the study of Li *et al.*,[13] GO showed the gas adsorption which followed the sequence of $CO_2 > CH_4 > N_2 > H_2$. Therefore, the membranes adsorption properties can be effectively tailored by the amount of oxygenated groups. As shown in Fig. 3b, different membranes were tested for specific adsorption of CO_2 and N_2. CO_2 adsorption capability was significantly enhanced with the GO O/C ratios, while N_2 was hardly adsorbed in all these membranes (Fig. S8†). This is because of the favorable interactions between the polar groups on GO nanosheets (such as –COOH and –OH) and CO_2

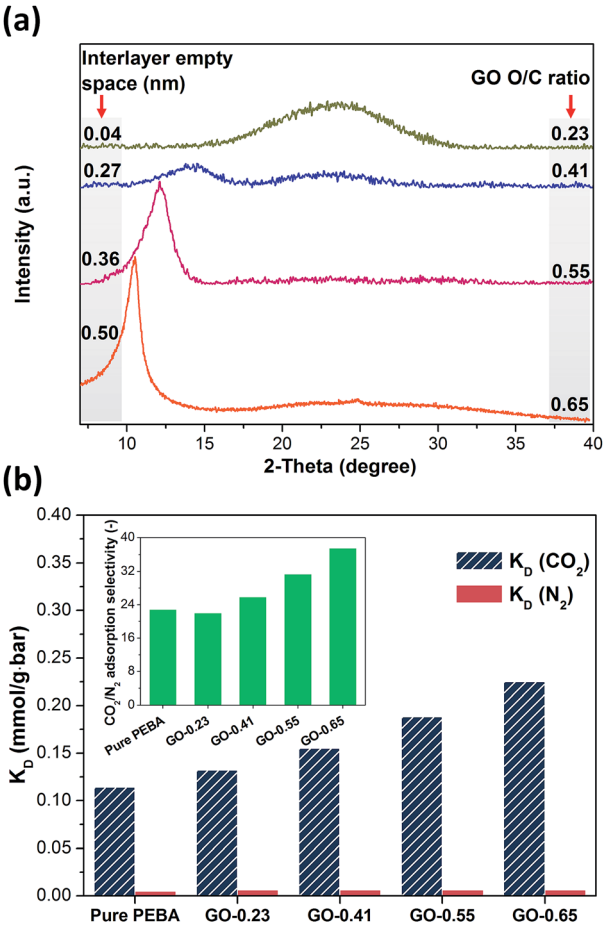

Fig. 3 (a) XRD patterns for GO with different O/C ratios. (b) Comparison of pure-component CO_2 and N_2 adsorptions (temperature: 25 °C, pressure: 0–1 atm) on membranes containing GO with different O/C ratios. See the detailed data in Fig. S9 (ESI†). The adsorption of all the membranes follow single-site Langmuir models, K_D is Henry's constant. Inserted is the comparison of CO_2/N_2 adsorption selectivity.

molecules.[14] GO-0.65 membrane exhibited the strongest CO_2 adsorption ability, which was 1.64 times that of pure PEBA membrane. It can be found that GO nanosheets endowed the GO–PEBA membrane with preferential CO_2 adsorption and transport, which is important for creating fast and selective nanochannels for CO_2 molecules.

The as-prepared membranes were further studied by gas permeation tests with H_2, CO_2, N_2 and CH_4. Fig. 4 shows distinct gas permeation behaviors of membranes containing GO with different O/C ratios. Compared with the tortuous pathways through parallel-stacked pure GO membranes, this type of nanocomposite membrane with inclined and even vertical GO stacks provides more straight and upright pathways, exhibiting much shorter transport distance.[17] As a result, gas molecules with appropriate dynamic diameter and affinity with GO can transport fast in the assembled 2D nanochannels. It can be seen that CO_2 molecules diffuse much faster than other gases, which is owing to its preferential adsorption and diffusion properties. A dramatic growth of CO_2 permeability

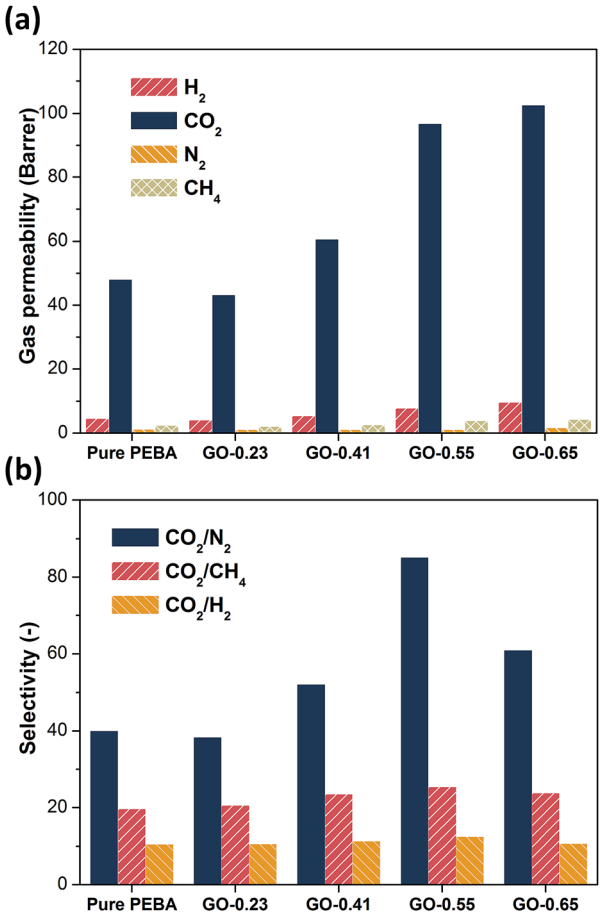

Fig. 4 Gas permeation behaviors of membranes containing GO with different O/C ratios. (a) Permeability of H_2, CO_2, N_2 and CH_4. (b) Selectivity of CO_2/N_2, CO_2/CH_4 and CO_2/H_2. Gas permeation tests were measured at 0.3 MPa and 25 °C, 1 barrer = 10^{-10} cm^3 (STP) cm cm^{-2} s^{-1} $cmHg^{-1}$.

occurred from GO-0.41 to GO-0.55 membrane (increased about 60%) with the increasing of GO interlayer spacing from 0.27 to 0.36 nm (Fig. 3a). In addition, the gas selectivity of CO_2/N_2 also increased obviously when O/C ratio of GO increased to 0.55. That is because that CO_2 molecules with kinetic diameter of 0.33 nm can transport more fast and selectively in GO-derived nanochannels with interlayer height of 0.36 nm than in polymer environment.[17,20] N_2 molecules with kinetic diameter of 0.364 nm can hardly travel through the confined space between the GO layers. Although the kinetic diameter of CH_4 (0.38 nm) is even larger than that of N_2, the selectivity of CO_2/CH_4 did not increased much. It is due to the fact that GO can also adsorb CH_4 molecules.[13] On the basis of the solution-diffusion theory,[24] the permeability of CH_4 also increased when incorporating GO nanosheets. When O/C ratio rose to 0.65, all the tested gases showed continued increase of permeability while the gas selectivity including CO_2/N_2, CO_2/CH_4 and CO_2/H_2 dropped, indicating the weakening of molecular sieving effect of GO nanochannels with large size (0.50 nm). In addition, membranes containing GO with low O/C ratio showed decreased selectivity compared with GO-0.55 membrane (Fig. 4b). It is due to that gas diffusion in as-prepared membrane was hindered when GO laminates were with a low content of oxygen-containing groups, because of the poor dispersibility and even aggregation of GO caused by the weak hydrogen bonding frameworks (Fig. S6 and S7†). Actually, this led to gas barrier effect since the CO_2 permeability of GO-0.23 was even lower than that of pure PEBA membrane. Moreover, the microdefects gradually generated during reduction process (Fig. S9†) also caused nonselective gas permeation, leading to decrease of gas selectivity. The comparison of gas permeation mechanisms is presented in Fig. 1 and further discussed in ESI,† which demonstrates the dominate effect of GO oxygenated groups. Future research should be carried out to effectively increase the amount of GO nanochannels without agglomeration, so as to obtain better separation performance.

As shown in Fig. 5, compared with pure PEBA membrane, the GO-0.55 membrane showed both significantly enhanced CO_2 permeability and selectivity, breaking the traditional "trade-off" relationship.[25,26] Also, the GO-0.55 membrane exhibited highest separation performance of CO_2/N_2 (CO_2 permeability: 97 barrer, CO_2/N_2 selectivity: 86), surpassing the upper-bound for state-of-the-art membranes, such as zeolite,[27] silica,[27] CMS,[28] pure GO,[29] PIM[30] as well as MOF-based membranes.[31–33] It is demonstrated that the oxygen-containing groups can finely manipulate the size of GO nanochannels and CO_2 adsorption behaviors, thus, endow the as-prepared membrane with highly efficient CO_2 separation performance, which offers promising potential for practical implementation of CO_2 capture.

In summary, the role of the oxygenated groups of graphene oxide (GO) for elaborately tailoring GO-derived nanochannels was demonstrated in this work. We found that GO with high content of oxygen-containing groups can show better dispersibility in polymeric environment and stronger hydrogen bonding frameworks between GO and polymer chains. Moreover, the size of GO-derived nanochannels and the adsorption properties were simultaneously influenced by controllable removing oxygenated groups on GO. The assembled GO

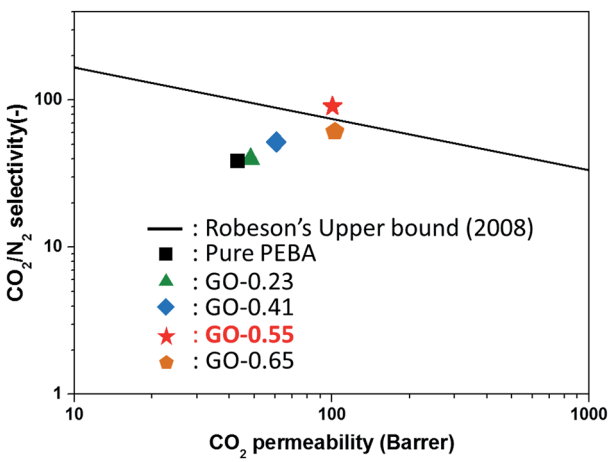

Fig. 5 CO_2/N_2 separation performances of as-prepared membranes compared with upper bound limit.

laminates with appropriate O/C ratio of 0.55 can provide sub-nanometer interlayer nanochannels (0.36 nm) with CO_2-philic properties for preferential permeation of CO_2 molecules. The as-prepared membrane exhibited excellent CO_2/N_2 separation performance, transcending upper-bound for state-of-the-art membranes, which is promising for CO_2 capture. Moreover, this study also deepens the understanding of the molecular transport mechanisms in confined nanochannels and provides new insights in designing flexible and large-area 2D nanomaterials-based films and devices applied for nanofluidic, catalytic and related fields.

Acknowledgements

This work was financially supported by the National Natural Science Foundation of China (Grant No. 21476107, 21490585, 21406107), the Innovative Research Team Program by the Ministry of Education of China (Grant No. IRT13070) and Top-notch Academic Programs Project of Jiangsu Higher Education Institutions (TAPP).

Notes and references

1 G. Liu, W. Jin and N. Xu, *Chem. Soc. Rev.*, 2015, **44**, 5016–5030.
2 D. A. Dikin, S. Stankovich, E. J. Zimney, R. D. Piner, G. H. B. Dommett, G. Evmenenko, S. T. Nguyen and R. S. Ruoff, *Nature*, 2007, **448**, 457–460.
3 W. S. Hummers and R. E. Offeman, *J. Am. Chem. Soc.*, 1958, **80**, 1339.
4 R. R. Nair, H. A. Wu, P. N. Jayaram, I. V. Grigorieva and A. K. Geim, *Science*, 2012, **335**, 442–444.
5 R. K. Joshi, P. Carbone, F. C. Wang, V. G. Kravets, Y. Su, I. V. Grigorieva, H. A. Wu, A. K. Geim and R. R. Nair, *Science*, 2014, **343**, 752–754.
6 K. Huang, G. Liu, Y. Lou, Z. Dong, J. Shen and W. Jin, *Angew. Chem., Int. Ed.*, 2014, **53**, 6929–6932.
7 K. Huang, G. Liu, J. Shen, Z. Chu, H. Zhou, X. Gu, W. Jin and N. Xu, *Adv. Funct. Mater.*, 2015, **25**, 5809–5815.
8 P. Sun, H. Liu, K. Wang, M. Zhong, D. Wu and H. Zhu, *Chem. Commun.*, 2015, **51**, 3251–3254.
9 H. Huang, Z. Song, N. Wei, L. Shi, Y. Mao, Y. Ying, L. Sun, Z. Xu and X. Peng, *Nat. Commun.*, 2013, **4**, 2979–2987.
10 S. J. Gao, H. Qin, P. Liu and J. Jin, *J. Mater. Chem. A*, 2015, **3**, 6649–6654.
11 D. L. Gin and R. D. Noble, *Science*, 2011, **332**, 674–676.
12 M. Hu and B. Mi, *Environ. Sci. Technol.*, 2013, **47**, 3715–3723.
13 H. Li, Z. Song, X. Zhang, Y. Huang, S. Li, Y. Mao, H. J. Ploehn, Y. Bao and M. Yu, *Science*, 2013, **342**, 95–98.
14 H. W. Kim, H. W. Yoon, S.-M. Yoon, B. M. Yoo, B. K. Ahn, Y. H. Cho, H. J. Shin, H. Yang, U. Paik, S. Kwon, J.-Y. Choi and H. B. Park, *Science*, 2013, **342**, 91–95.
15 C. Cheng, G. Jiang, C. J. Garvey, Y. Wang, G. P. Simon, J. Z. Liu and D. Li, *Sci. Adv.*, 2016, **2**, e1501272.
16 W.-S. Hung, C.-H. Tsou, M. De Guzman, Q.-F. An, Y.-L. Liu, Y.-M. Zhang, C.-C. Hu, K.-R. Lee and J.-Y. Lai, *Chem. Mater.*, 2014, **26**, 2983–2990.
17 J. Shen, G. Liu, K. Huang, W. Jin, K.-R. Lee and N. Xu, *Angew. Chem., Int. Ed.*, 2015, **54**, 578–582.
18 J. Shen, G. Liu, K. Huang, Z. Chu, W. Jin and N. Xu, *ACS Nano*, 2016, **10**, 3398–3409.
19 A. Lerf, H. He, M. Forster and J. Klinowski, *J. Phys. Chem. B*, 1998, **102**, 4477–4482.
20 M. Karunakaran, R. Shevate, M. Kumar and K. V. Peinemann, *Chem. Commun.*, 2015, **51**, 14187–14190.
21 W. Gao, L. B. Alemany, L. Ci and P. M. Ajayan, *Nat. Chem.*, 2009, **1**, 403–408.
22 N. I. Kovtyukhova, T. E. Mallouk, L. Pan and E. C. Dickey, *J. Am. Chem. Soc.*, 2003, **125**, 9761–9769.
23 X. Huang, X. Qi, F. Boey and H. Zhang, *Chem. Soc. Rev.*, 2012, **41**, 666–686.
24 D. F. Sanders, Z. P. Smith, R. Guo, L. M. Robeson, J. E. McGrath, D. R. Paul and B. D. Freeman, *Polymer*, 2013, **54**, 4729–4761.
25 L. M. Robeson, *J. Membr. Sci.*, 2008, **320**, 390–400.
26 B. D. Freeman, *Macromolecules*, 1999, **32**, 375–380.
27 D. Shekhawat, D. R. Luebke and H. W. Pennline, *A Review of Carbon Dioxide Selective Membranes*, US department of energy, 2003.
28 H. Park and Y. Lee, *Adv. Mater.*, 2005, **17**, 477–483.
29 H. W. Kim, H. W. Yoon, S.-M. Yoon, B. M. Yoo, B. K. Ahn, Y. H. Cho, H. J. Shin, H. Yang, U. Paik and S. Kwon, *Science*, 2013, **342**, 91–95.
30 N. Du, H. B. Park, G. P. Robertson, M. M. Dal-Cin, T. Visser, L. Scoles and M. D. Guiver, *Nat. Mater.*, 2011, **10**, 372–375.
31 Q. Song, S. K. Nataraj, M. V. Roussenova, J. C. Tan, D. J. Hughes, W. Li, P. Bourgoin, M. A. Alam, A. K. Cheetham, S. A. Al-Muhtaseb and E. Sivaniah, *Energy Environ. Sci.*, 2012, **5**, 8359–8369.
32 H. Gong, T. H. Nguyen, R. Wang and T.-H. Bae, *J. Membr. Sci.*, 2015, **495**, 169–175.
33 N. C. Su, D. T. Sun, C. M. Beavers, D. K. Britt, W. L. Queen and J. J. Urban, *Energy Environ. Sci.*, 2016, **9**, 922–931.